Thesis for the Degree
Master of Education

XPS Investigation of Room Temperature Ionic Liquids in UHV

by

Ji Hye Kwon

Graduate School of Education

Pukyong National University

August 2007

XPS Investigation of Room Temperature Ionic Liquids in UHV

초고진공에서의 상온 이온성 액체의 X-선 광전자 분광학 연구

Advisor : Prof. Yong-Cheol Kang

by

Ji Hye Kwon

A thesis submitted in partial fulfillment of the requirements
for the degree of

Master of Education

Graduate School of Education
Pukyong National University

August 2007

XPS Investigation of Room Temperature Ionic Liquids in UHV

A dissertation

by

Ji Hye Kwon

Approved by :

Chairman : Ju Chang Kim

Member : So Won Youn

Member : Yong-Cheol Kang

August 30, 2007

Contents

List of Figures

List of Tables

XPS Investigation of Room Temperature Ionic Liquids in UHV

Ji Hye Kwon

Graduate School of Education
Pukyong National University

Abstract

A new analytical application of XPS to the identification of organic molecules in a room temperature ionic liquid has been studied. An organic compound, propargylamine (**1**), produced in 1-butyl-3-methylimidazolium hexafluorophosphate ([bmim][PF_6]), which is one of the room temperature ionic liquids (RTILs), via A^3 coupling reaction, was characterized by means of x-ray photoelectron spectroscopy (XPS) rather than using conventional organic compound analysis techniques such as nuclear magnetic resonance (NMR). There are four non-equivalent carbons in the RTIL and **1** each. The ratios of integrated areas of the deconvoluted peaks of core electron of carbon (C1s) are well matched to the number of carbons in those compounds. The binding energies of C1s of the featured carbons in **1**, C4 (sp carbons in acetylene group) and C5 (sp^2 carbons in benzene ring), were assigned 286.2 and 285.4 eV, respectively. Some pure RTILs were also characterized by using XPS in Ultra High Vacuum (UHV). These results may provide an important tool and a new strategy for the analysis of organic molecules.

Ⅰ. Introduction

X-ray photoelectron spectroscopy (XPS) is a surface analysis technique in huge range of solid samples that provides information about identification of elemental composition and verification of chemical environments of atoms [1,2]. The XPS analysis requires Ultra High Vacuum (UHV) environment for minimum interference from gas phase scattering since the signal from the surface is very weak. Unfortunately, this XPS analysis environment enables us not to make experiment for most of liquid samples becoming easily evaporation in comparison solid samples with low vapor pressure. It has been tried variety methods of XPS analysis for liquid samples in UHV [3] regardless of difficulty; micro liquid jet [4,5], differential pumping [6], controlled adsorption [7], freeze-drying [8,9] and fast-freezing [10,11]. However, the previous methods are complicated than general method of analysis process for solid samples, that are not easy to use.

Recently, some researches showed that these analytical difficulty was solved by using Room Temperature Ionic Liquids (RTILs) [12-21]. RTILs have extremely low vapor pressure, therefore, this materials have not evaporated easily in UHV! Besides, a variety of organic reactions, transition metal-catalyzed reactions, and biotransformations have been extensively studied in RTILs [20-23] and many analytical applications were applied to characterize RTILs systems [24-29]. RTILs are very fascinating reaction media against conventional organic solvents due to their unique properties such as non-detectable vapor pressure, environmental safety, reusability, reasonable thermal stability, polarity, and good solubility for organic, inorganic, and organometallic compounds [30-32]. These characteristics of RTILs perfectly satisfy the criteria for using XPS to monitor catalytic organic reactions in RTILs.

In this thesis, the two experimental data are reported. First, propargylamine (**1**) was synthesized through A^3 coupling reaction among (alkyne (phenylacetylene), aldehyde (benzaldehyde) and amine (piperidine)) in 1-*n*-butyl-3-methyl-imidazolium hexafluorophosphate, [bmim][PF_6] [33], then the reaction was monitored using XPS in UHV condition without any treatments. Second, some pure RTILs were analyzed using XPS in UHV.

Herein a new field for identification of organic compounds in RTILs, is reported and results of pure RTILs were characterized using XPS are reported also.

Ⅱ. Theory

1. The basis for XPS

XPS is based on the photoelectric effect. The surface to be analyzed is first placed in a vacuum environment and then irradiated with photons. For XPS, the phton source is in the X-ray energy range. The atoms comprising the surface emit electrons (photoelectrons) after direct transfer of energy from the photon to the core-level electron. These emitted electrons are subsequently separated according to energy and counted. The energy of the photoelectrons is related to the atomic and molecular environment from which they originated. The number of electrons emitted is related to the concentration of the emitting atom in the sample [1].

The physical basis of the XPS technique is shown in Figure 1. When a core electron is ejected by a photon of energy $h\nu$, the kinetic energy E_K of emitted photoelectron is :

$$E_K = h\nu - E_B - \phi$$

where E_K (the experimental quantity measured by the spectrometer) is referenced to a core electron of binding energy E_B (an intrinsic material property) and work function of the solid ϕ, is related to the vacuum level the specimen, $E_{V,}$ and the Fermi level, $E_{F,}$ (the outermost electrons of the solid from a band) by: $\phi = E_F - E_V$ [36,38]

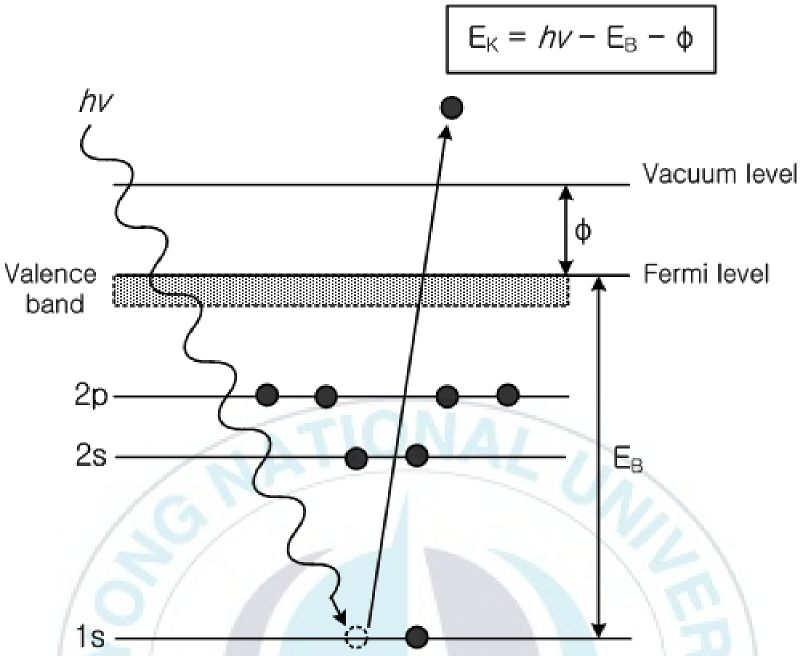

Figure 1. The X-ray photon transfers its energy to a core-level electron imparting enough energy for the electron to leave the atom.

2. The instrumentation for XPS

The XPS experiment is necessarily tied to the complex instrumentation needed to stimulate photoemission and to measure low fluxes of electrons. A schematic drawing of XPS instrument is shown in Figure 2. The primary components that make up the XPS instrument are the vacuum system, X-ray source, electron energy analyzer, and data system [1].

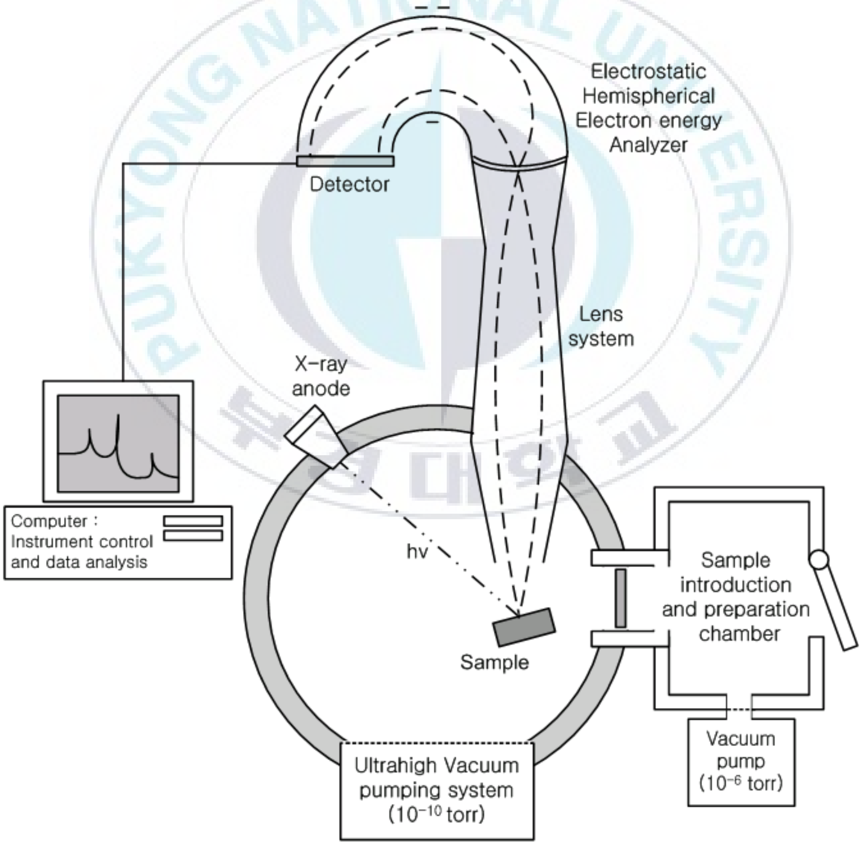

Figure 2. Schematic arrangement of a photoelectron spectrometer.

2.1. Vacuum system

The heart of the XPS instrument is the main vacuum chamber where the sample is analyzed. The XPS experiment must be done under vacuum for three reasons. First, the emitted photoelectrons must be able to travel from the sample through the analyzer to the detector without colliding with gas phase particles. Second, some components such as the X-ray source require vacuum conditions to remain operational condition. Third, the surface composition of the sample under investigation must not change during the XPS experiment. Only a modest vacuum (10^{-6} ~ 10^{-7} torr; 1 torr = 133 Pa) is necessary to meet the first two requirements. More stringent vacuum conditions are necessary to avoid contamination of the sample. The actual vacuum required will depend on the reactivity of the sample. For most applications a vacuum of 10^{-10} torr is adequate [1].

2.2. X-ray sources

Figure 3 shows the twin-anode X-ray source. X-ray is generated by bombardment of anode material with high-energy electrons. The electrons are emitted from a tungsten filament are accelerated (15 kV) and focussed onto a water-cooled anode. Anodes are usually water-cooled, because the photon flux is proportional to the electron current striking the anode and the maximum anode current is determined by the efficiency with which the heat can be dissipated. The aluminium window is necessary in order to screen the sample from stray electrons, heating effects and any contamination originating in the source [2].

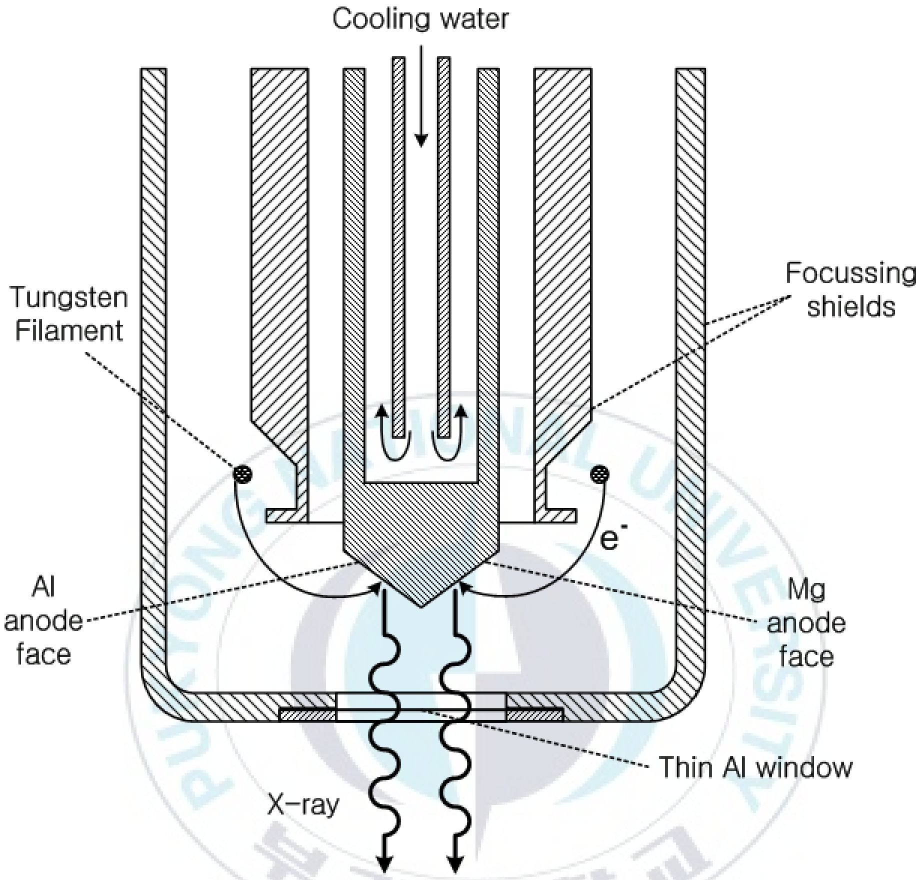

Figure 3. Twin anode (Mg/Al) X-ray source.

The Table 1 lists commonly available emission line, energy and full-width half maximum (FWHM) of anode material.

Anode material	Emission line	Energy (eV)	Full-Width Half Maximum (eV)
Y	$M\zeta$	132.3	0.47
Zr	$M\zeta$	151.4	0.77
Mg	$K\alpha_{1,2}$	1253.6	0.7
Al	$K\alpha_{1,2}$	1486.6	0.9
Si	$K\alpha$	1739.6	1.0
Zr	$L\alpha$	2042.4	1.7
Ag	$L\alpha$	2984.4	2.6
Ti	$K\alpha$	4510.9	2.0
Cr	$K\alpha$	5417.0	2.1

Table 1. Characteristic energies and FWHMs for common anode materials for XPS.

The choice of anode material for XPS, must be high enough photon energy to excite an intense photoelectron peak from all elements, and also possess a natural X-ray line width that will not broaden the resultant spectrum excessively (less then 1.0 eV). Thus the two materials used universally as anodes in X-ray sources are magnesium and aluminium. The twin-anode design shown in Figure 3 is popular and enables either Mg or Al $K\alpha$ X-rays [37]. Such twin anode assembles are useful as they provide a modest depth profiling capability and the ability to differentiate between Auger and photoelectron transition when the two overlap in one radiation [36].

2.3. Electron energy analyzer

The analyzer system consists of three components: the collection lens, the energy analyzer and detector. Figure 4 shows the schematic diagram of electron energy analyzer for XPS.

The lens system can increase collection angle that degrade upon exposure to X-rays, since the more efficient the detection system is the more data that can be collected before the sample is damaged. The lens system also retards E_K of electrons, because they are ejected from the sample is usually too great for the analyzer to produce sufficiently high resolution. The lens system moves the analyzer away from the analysis position allowing other components of the spectrometer to be placed closer to the sample [1,36].

Most common type of electrostatic deflection-type analyzer for XPS called the concentric hemispherical analyzer (CHA). It consists of two concentric hemispheres of radius R_1 (inner) and R_2 (outer). A potential difference of ΔV is placed across the two hemispheres with the outer hemisphere (V_2) being more negative than the inner one (V_1). An electron of kinetic energy V_0 will travel a circular orbit through hemispheres at radius R_0=(R_1+R_2/2). The relationship between V_1, V_2 and V_0 is given by

$$V_0 = \frac{V_1 R_1 + V_2 R_2}{2R_0}$$

Since $R_{0,}$ R_1 and R_2 are fixed, in principle changing V_1 and V_2 will allow scanning of electron E_K following mean path through hemispheres. The electrons are deflected by an electrostatic field. There is a range of electron energies that can successfully travel from the entrance to the exit of the analyzer without undergoing a collision with one of the hemispheres.

The passed electrons through the energy analyzer arrive at the detector and count the individual electrons. Detector consist of a spiral-shaped glass tube with a conical collector at one end and a metal anode at the other. The internal walls of detector are coated with a excellent resistance material which will emit many secondary electrons. The electron pulse is amplified further and counted by standard counting electronics [38].

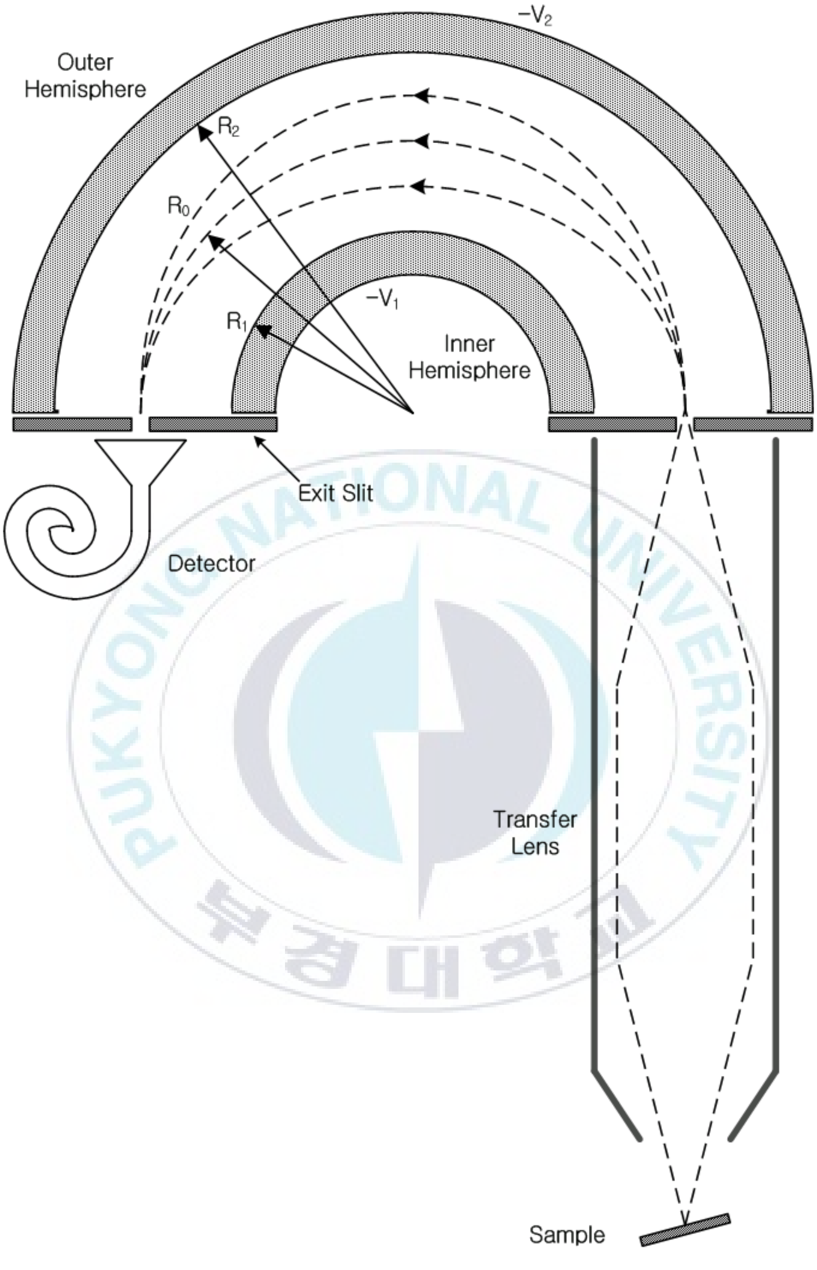

Figure 4. Diagram of a CHA with standard input lens systems, analyzer and detector for XPS.

2.4. Deconvolution

To maximize the information extracted from XPS spectra, the peak area and E_B of each subpeak for a given orbital must be determined. Typically, individual subpeaks, due to chemical environment, are not completely separated in an experimental spectrum. This requires the use of a deconvolution procedure to resolve the desired peak parameters. Quantities used in such procedures include the background, peak shape, peak position, peak height, and peak width. After the background has been determined, initial guesses are made for each peak parameter and then a least-squares fitting routine is used to iterate to the final values. Caution must be exercised when performing the peak fit since many of the quantities are correlated. In cases like this, there is no substitute for experience gained while working on the data system with real results to analyse. Under these conditions all peaks should have similar widths. Generally a Gaussian peak shape is being used for the resolution term together with a combination of two Lorentzian functions to simulate the line shape contribution [36,38].

3. Room temperature ionic liquids

What are ionic liquids? Quite simply, they are liquids that are composed entirely of ions. Molten sodium chloride, for example, is an ionic liquid but a solution of sodium chloride in water is an ionic solution. The term molten salts evokes an image of high-temperature, viscous and highly corrosive media. The term ionic liquid, in contrast, implies a material that is fluid at (or close to) ambient temperature with a low viscosity and is easily handled, i.e. a material with attractive properties for a solvent. Room temperature ionic liquids are generally salts of organic cations, e.g. tetraalkylammonium, tetraalkylphosphonium, *N*-alkylpyridinium, 1,3-dialkylimidazolium and trialkylsulfonium cations (Figure 5).

Cations	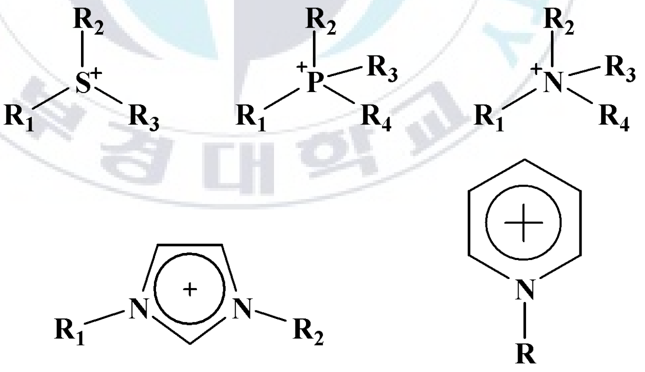
Anions	BF_4^-, PF_6^-, SbF_6^-, NO_3^-, $CF_3SO_3^-$, $(CF_3SO_3)_2N^-$, $ArSO_3^-$, $CF_3CO_2^-$, $CH_3CO_2^-$, $Al_2Cl_7^-$

Figure 5. Molecular structures of ionic liquids.

In order to be liquid at room temperature, the cation should preferably be unsymmetrical, e.g. R_1 and R_2 should be different alkyl groups in the dialkylimidazolium cation. The melting point is also influenced by the nature of the anion (see Table 2) [39].

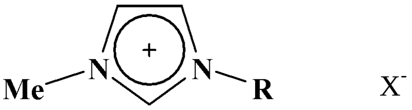

R	**X**	**mp/℃**
Me	Cl	125
Et	Cl	87
n-Bu	Cl	65
Et	NO_3	38
Et	$AlCl_4$	7
Et	BF_4	6
Et	CF_3SO_3	-9
Et	$(CF_3SO_3)_2N$	-3
Et	CF_3CO_2	-14
n-Bu	CF_3SO_3	16

Table 2. Melting points of some dialkylimidazolium salts.

Recently, Room Temperature Ionic Liquids (RTILs) have attracted much attention for their excellent properties such as wide temperature range of the liquid phase, excellent chemical and thermal stabilities, very low vapor pressure, good electrical conductivity and high ionic mobility [40-44].

Ⅲ. Experimental

1. Preparation of sample

1.1. A^3 coupling reaction

A^3 coupling (three-component coupling of aldehydes, alkynes and amines) was carried out as follows. A mixture of [bmim][PF_6] (1 mL) and CuI (1.9 mg, 0.01 mmol, 2 mol% as a catalyst) was degassed under reduced pressure at 80 ^oC for 30 min, and then N_2 was introduced. To the solution were added piperidine (75 µL, 0.75 mmol), benzaldehyde (51 µg, 0.5 mmol) and phenylacetylene (67 µL, 0.6 mmol), and the resulting mixture was heated at 120 ^oC for 2 h with stirring. The reaction mixture was cooled and extracted with diethyl ether (5 mL, 5 times). The combined organic layer was concentrated and the crude mixture was purified by flash chromatography on silica gel with eluent of *n*-hexane-ethyl acetate (10:1). For tracking the reaction profile, 100 µL aliquots were taken from the reaction vessels every 15 minutes.

Figure 6 shows the mechanism of A^3 coupling reaction employed in this investigation. A tentative mechanism was proposed involving the activation of the C-H bond of alkyne by Cu(Ⅰ). The copper acetylide (phenylacetylide) intermediate thus generated reacted with the iminium ion generated *in situ* from aldehydes (benzaldehyde) and secondary amines (piperidine) to give the corresponding propargylamine and regenerate the Cu(Ⅰ) catalyst for further reactions [45].

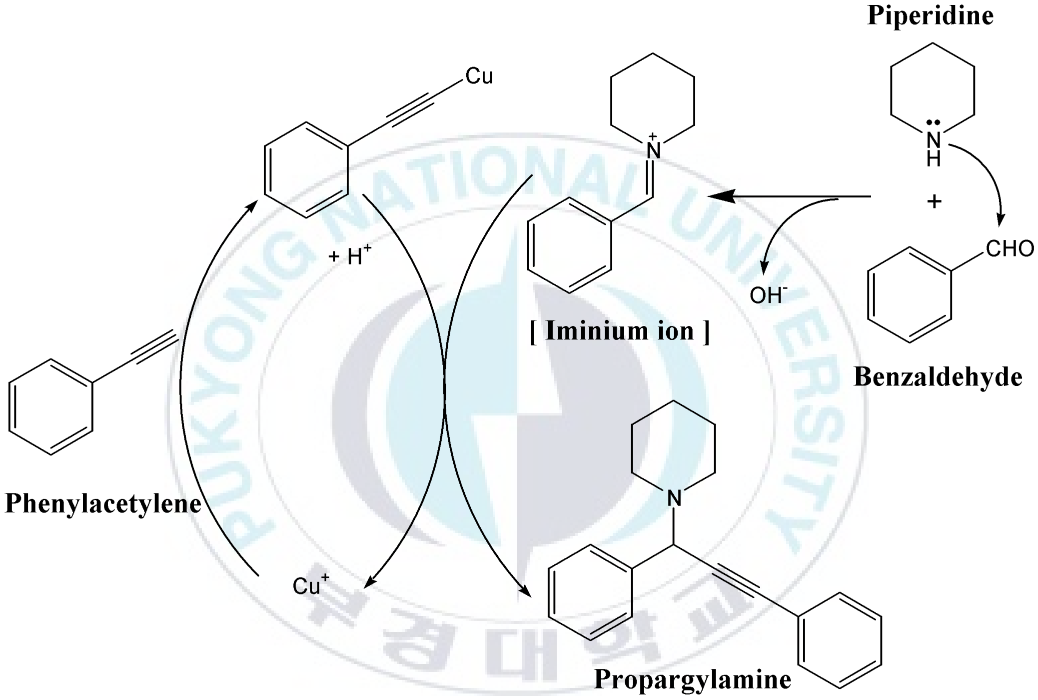

Figure 6. Mechanism of A^3 coupling reaction.

1.2. Pure RTILs study

In this experiment, using pure RTILs without any other treatment were [bmim][PF_6], [bmim][BF_4], [bmim][OTf] and [emim][BF_4]. The RTILs were dropped on the custom-made sample holder, and then put into the preparation chamber for two days for prepumping. Figure 7 shows the ordered sample holder for RTILs.

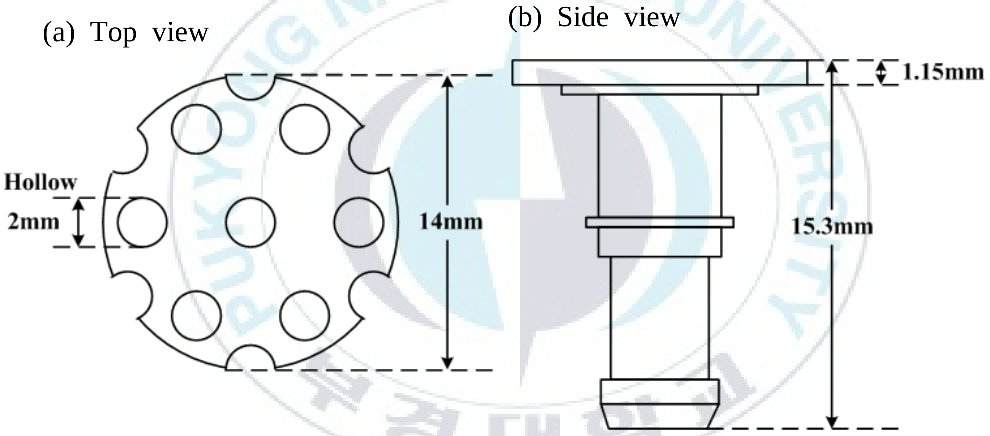

Figure 7. Custom-made sample holder for RTILs.

(a) top view (b) side view.

2. The operation of XPS

Monitoring of the reaction was carried out in an UHV chamber (base pressure 5x10^{-10} mbar) equipped with a CHA and a twin anode X-ray source (Mg/Al Kα 1253.6 and 1486.6 eV, respectively) for XPS (VG ESCALAB 2000). The XPS chamber was pumped by two stages of pumping system. The first one is that a turbomolecular pump (TMP) backed by a two stage rotary vane pump (RP) system pumps a fast entry air load-lock (FEAL) chamber. And the second system consists of an ion getter pump and a Ti-sublimation pump and evacuates analysis chamber to maintain UHV condition. An ion sputtering gun is equipped in the analysis chamber for sample cleaning and depth profile study. A charge-coupled device (CCD) camera guides to set up the sample for x-ray photoelectron analysis.

During survey scans, spectra were obtained using Mg Kα x-ray source. X-ray source was at high voltage of 15 kV, beam current of 15 mA, filament current of 4.2 A, pass energy of 50 eV, dwell time of 50 ms and energy step size of 1 eV in constant analyzer energy (CAE) mode at large area XPS (LAXPS). High resolution spectra were obtained at pass energy of 20 eV, energy step size of 0.05 eV and other factors were kept the same as survey scan. Under these conditions, aliphatic carbon 1s peak was corrected to 285 eV [14,46]. Each aliquot taken every 15 minutes from the start of the experiment is pre-pumped in the FEAL chamber for 2 hrs before loading into the analysis chamber which was pumped by a TMP (70 l/s) backed by an RP (200 l/min.).

3. Deconvolution

The XPS data were deconvoluted using XPSPEAK software (ver 4.1). Obtained XPS C1s peaks were divided into several peaks according to their chemical environments. The FWHM of each peak was between 1.2 and 1.9 eV, and G/L ratio of 30% (Lorentzian - 30 %, Gaussian - 70 %). χ^2 value (relationship between experimental peak and fitted curve) of all peaks fitted below 50.

Ⅳ. Results and Discussion

1. A^3 coupling reaction

Figure 8 shows the high resolution C1s XP spectra of pure [bmim][PF_6] and the product **1** of A^3coupling reaction in a RTIL by reaction time from the bottom. Even the RTILs are pure, the C1s XP spectra look like combining several peaks because there are four nonequivalent carbons in [bmim][PF_6]. The C1s peak around 285 eV is evoluted by the reaction time. This peak is caused by the carbons in benzene ring, which are the featured carbons of **1**. Figure 9 also shows high resolution N1s XP spectra. The evoluted N1s peak around 400 eV by reaction time is caused by the nitrogen of **1**. The details of the carbons and nitrogens of pure RTILs and **1** in solution of RTILs are shown in Figure 10 (a)-(b) and 11 (a)-(b), respectively.

In order to check whether the featured photoelectron of components signal comes from product or not, three RTILs solutions which contained same amount of reactants each (piperidine, phenylacetylene, benzaldehyde) were made and pumped in the FEAL chamber for 2 h same as the reacted aliquots prepumped. Bubbles were observed during prepumping process from the RTILs solutions with reactants. Figure 12 (a)-(c) show the C1s peaks of those samples. Very weak C1s photoelectron signal coming from the reactants were detected. This means that the unreacted reactants, which have relatively low boiling points, were almost evaporated in the FEAL chamber (low vacuum) before the aliquots were installed in the analysis chamber. In the analysis chamber, the low boiling point organic molecules completely evaporated. Therefore it can be ruled out that some featured C1s photoelectron signal in Figure 10 (b) came from the unreacted reactants. XPS analysis is sensitive enough to give us the chemical information of organic carbons in RTILs.

Figure 10 (a) and (b) show the detailed C1s XP spectra of pure [bmim][PF$_6$] and **1** in [bmim][PF$_6$], respectively. The normalized relative areas of nonequivalent C1s peaks were fixed by the stoichiometry of the [bmim][PF$_6$] and **1**. It was assigned that the binding energies of C1s photoelectron of each deconvoluted peak based on the chemical environment of the carbons [46]. The carbons according to the binding energy of C1s photoelectron from high to low were labeled. The aliphatic carbons (C6) are corrected to 285.0 eV [14]. The binding energy of C1 (287.9 eV) is assigned higher than that of C2 (287.4 eV) because the C2 hydrogen participates in hydrogen-bonding with hexafluorophosphate anion [47]. In Figure 10 (b), new featured peaks (C4 and C5; 286.2 and 285.4 eV, respectively) of **1** and larger peaks (C3 and C6; 286.7 and 285.0 eV) compared with C1s peaks of pure [bmim][PF$_6$] in Figure 10 (a) could be seen.

Figure 11 (a) and (b) show the detailed N1s XP spectra of pure RTILs and **1** in a RTIL respectively. In Figure 11 (b), new featured peak (N2 ; 400.34 eV) of **1** compared with N1s peaks of pure [bmim][PF_6] in Figure 11 (a) could be seen.

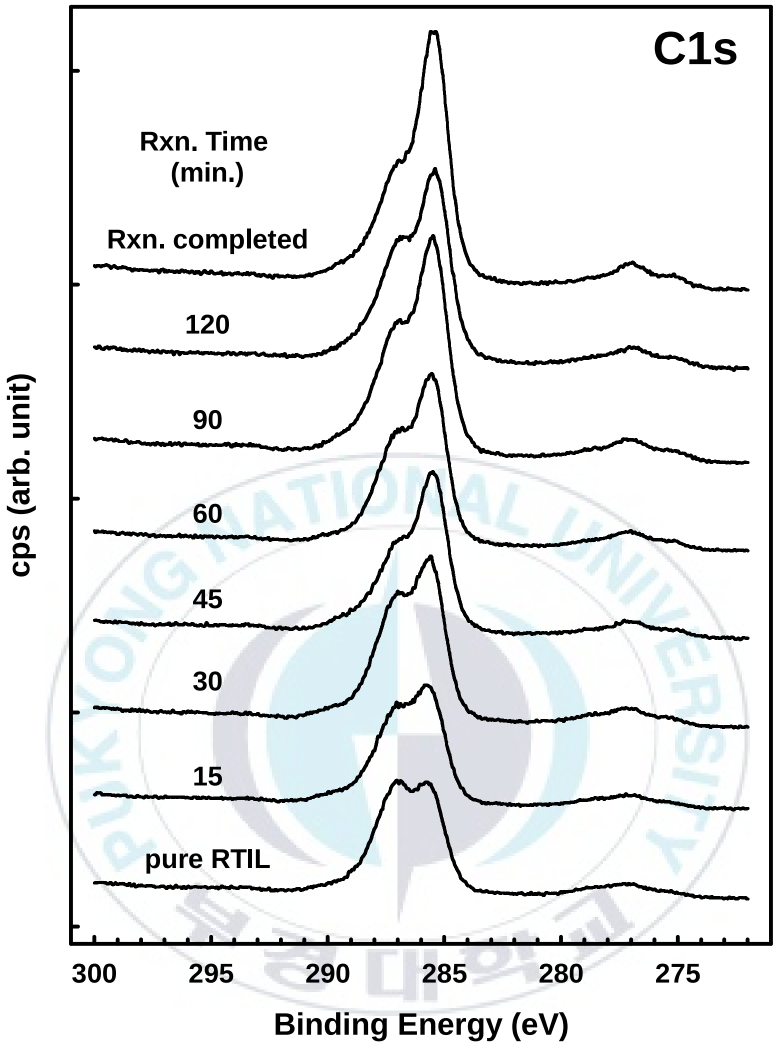

Figure 8. High resolution XP spectra of C1s photoemission of propargylamine (1) in [bmim][PF_6] by A^3 coupling (tree-component coupling of aldehydes, alkynes and amines) reaction time.

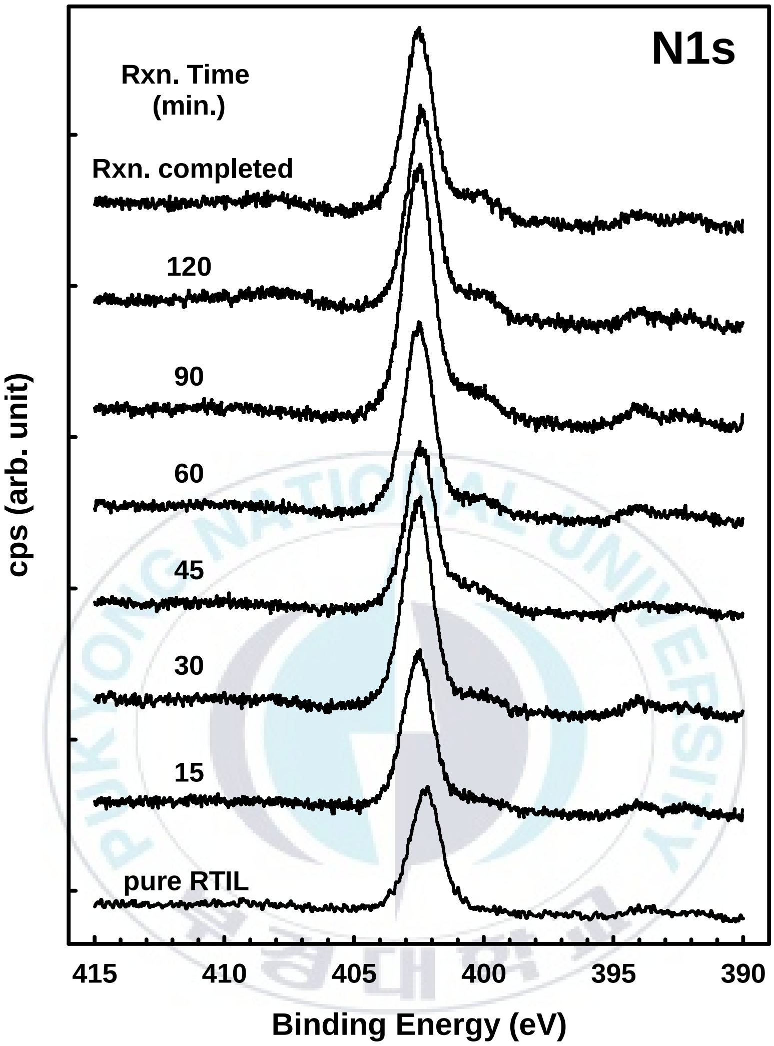

Figure 9. High resolution XP spectra of N1s photoemission of propargylamine (1) in [bmim][PF_6] by A^3 coupling reaction time.

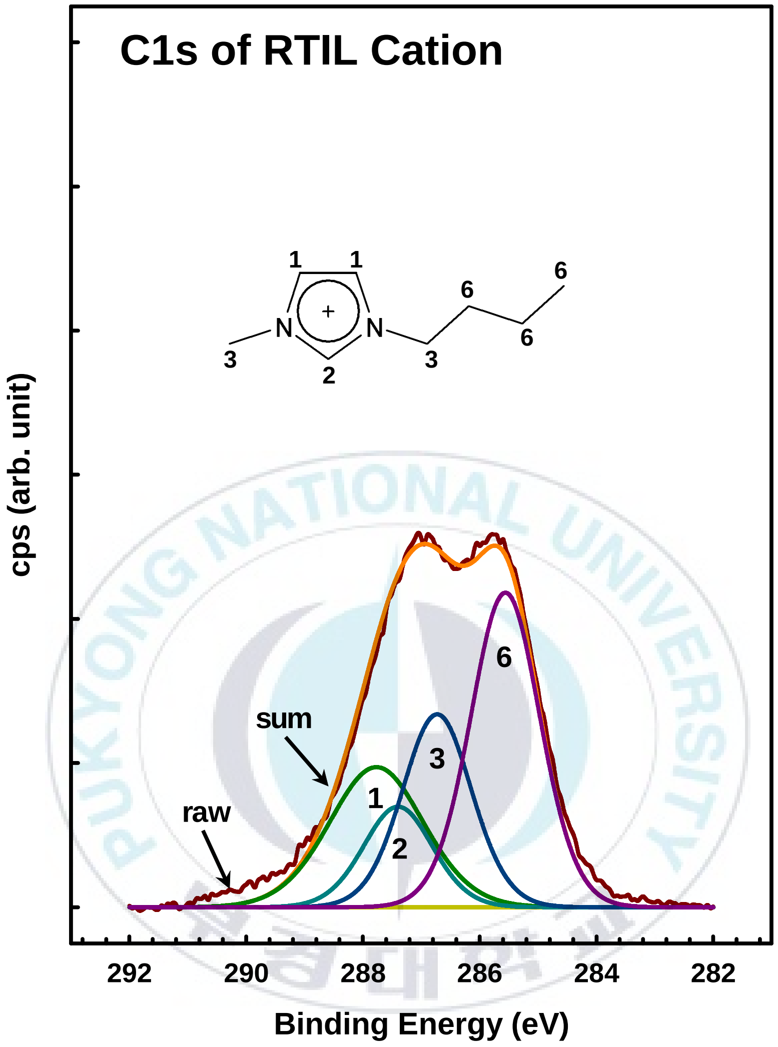

Figure 10. (a) Detailed C1s photoemission of pure 1-*n*-butyl-3-methylimidazolium cation. Top two peaks are sum of deconvoluted C1s (smooth line) and raw data (wiggled line). The inset shows the chemical structure of 1-*n*-butyl-3-methylimidazolium cation. (Area ratio 1.98:1.00:1.92:3.13)

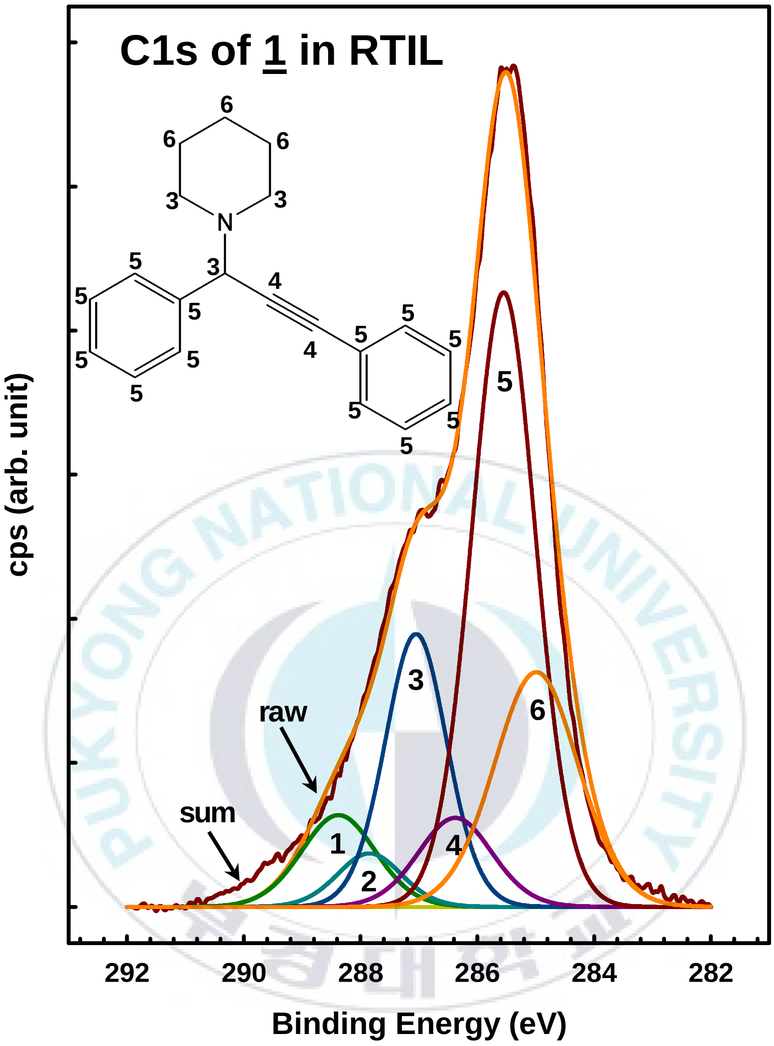

Figure 10. (b) Deconvoluted peaks of C1s photoelectron emission of propargylamine, 1, in a RTIL. The peaks labeled as C1 and C2 carbons are originated from RTIL and top two peaks are sum of deconvoluted C1s (smooth line) and raw spectra (wiggled line). The inset shows the molecular structure of the product, propargylamine, of the A^3 coupling reaction. (Area ratio 1.98:1.00:4.90:1.92:11.49:5.74)

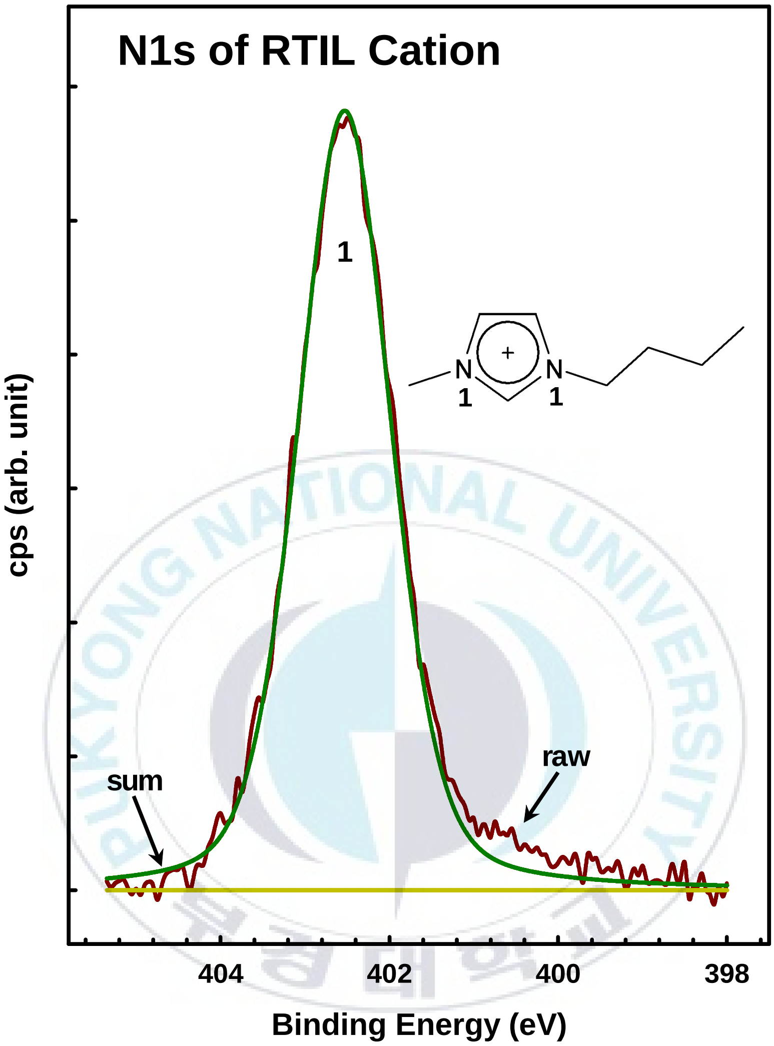

Figure 11. (a) Detailed N1s photoemission of pure 1-*n*-butyl-3-methylimidazolium cation. The inset shows the chemical structure of 1-*n*-butyl-3-methylimidazolium cation.

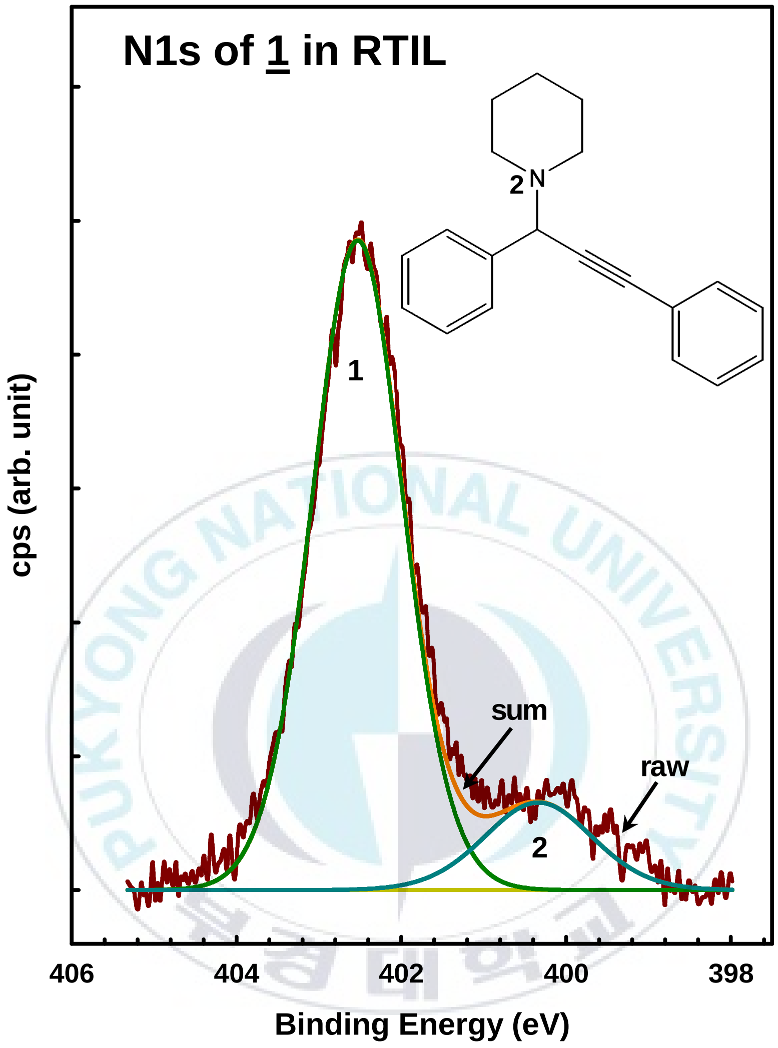

Figure 11. (b) Deconvoluted peaks of N1s photoelectron emission of propargylamine, **1**, in a RTIL. The peaks labeled as N2 nitrogen is originated from RTIL and top two peaks are sum of deconvoluted N1s (smooth line) and raw spectra (wiggled line). The inset shows the molecular structure of the product, propargylamine, of the A^3 coupling reaction.

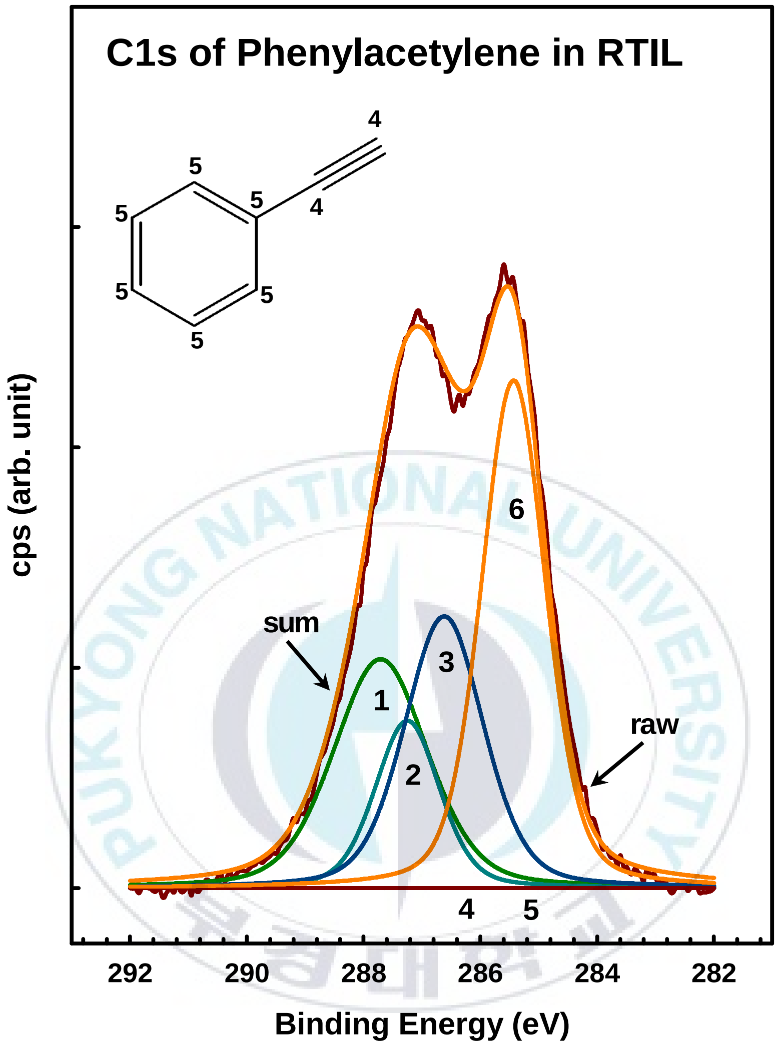

Figure 12. (a) Deconvoluted peaks of C1s photoelectron emission of phenylacetylene in a RTIL. The peaks labeled as C4 and C5 carbons are originated from reactant, phenylacetylene. The inset shows the molecular structure of the reactant, phenylacetylene, using in the A^3 coupling reaction. (Area ratio 2.00:1.00:2.00:0.00:0.00:3.03, boiling point = 144 ℃)

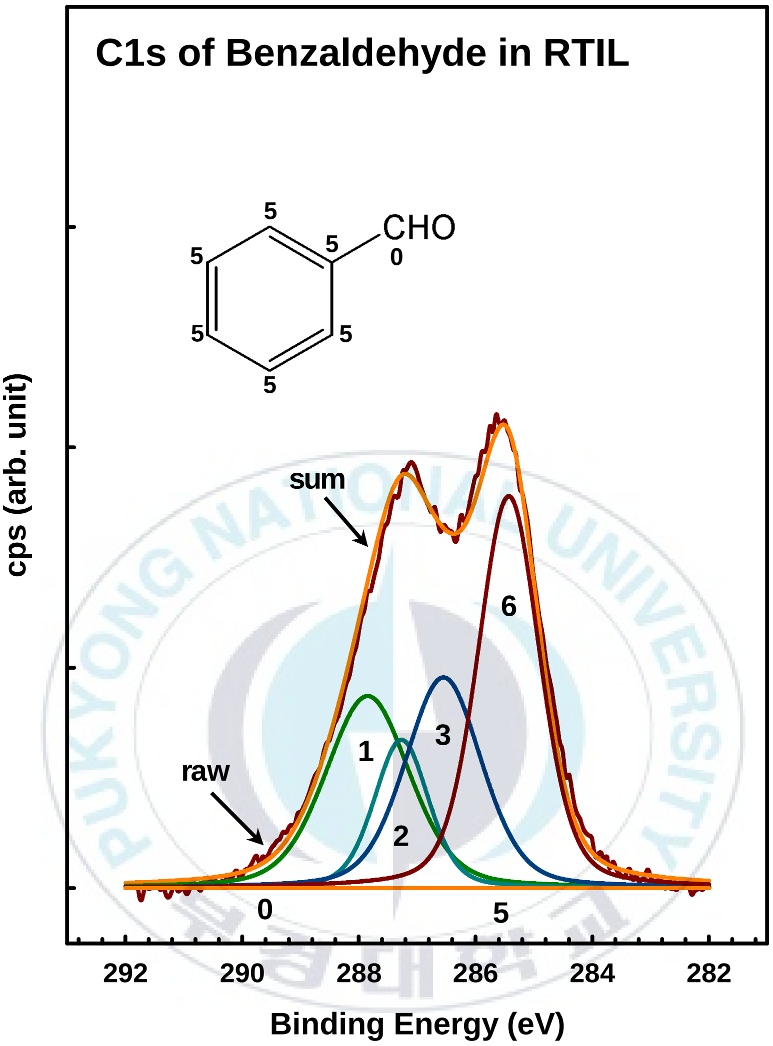

Figure 12. (b) Deconvoluted peaks of C1s photoelectron emission of benzaldehyde in a RTIL. The peaks labeled as C0 and C5 carbons are originated from reactant, benzaldehyde. The inset shows the molecular structure of the reactant, benzaldehyde, using in the A^3 coupling reaction. (Area ratio 0.00:2.00:1.00:2.00:0.00:3.00, boiling point = 179 ℃)

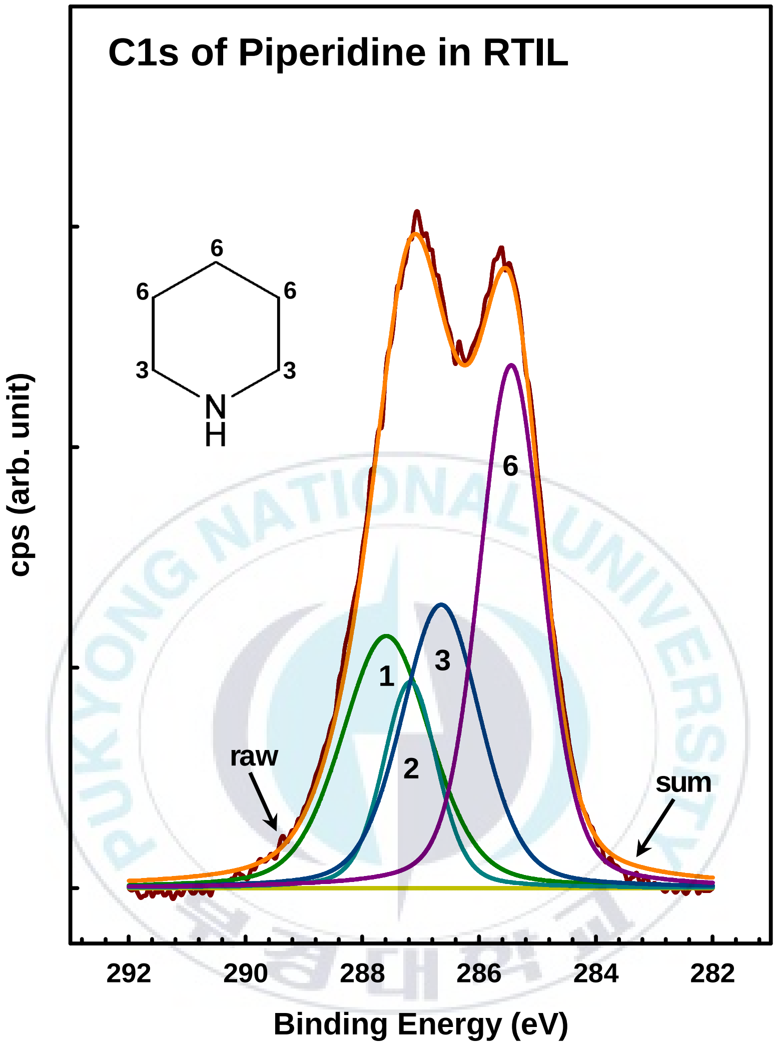

Figure 12. (c) Deconvoluted peaks of C1s photoelectron emission of piperidine in a RTIL. The peaks labeled as C3 and C6 carbons are originated from reactant, piperidine. The inset shows the molecular structure of the reactant, piperidine, using in the A^3 coupling reaction. (Area ratio 2.00:1.00:2.00:3.00, boiling point = 106 ℃)

Figure 13 shows the ratio of integrated areas of detailed C1s peaks in different chemical environment by the reaction time. There is only pure [bmim][PF_6] before the A^3 coupling reaction occurred (reaction time = 0). The ratio of integrated areas of carbons labeled 1:2:3:6 is 1.98:1.00:1.92:3.13. It was calculated peak area ratio after assuming that the photoelectron sensitivities of the carbons in organic compounds are same. This ratio from experimental results is well matched with the number of carbons in [bmim][PF_6], 2:1:2:3, within experimental error. As the A^3 coupling reaction progressed, the integrated areas of featured peaks of **1** (C4 and C5) and peaks of C3 and C6 increased gradually. The integrated areas of C3 and C6 are contributed from [bmim][PF_6] and **1**. After we subtracted the contribution of [bmim][PF_6] from the peak areas of XP spectra obtained from completed reaction, the ratio of integrated areas of carbons labeled 3:4:5:6 is 2.98:1.92:11.49:2.61 in the product in a RTIL solution. This ratio is close to the number of carbons in **1**, 3:2:12:3. This is the result to characterize an organic compound in a RTIL under UHV condition.

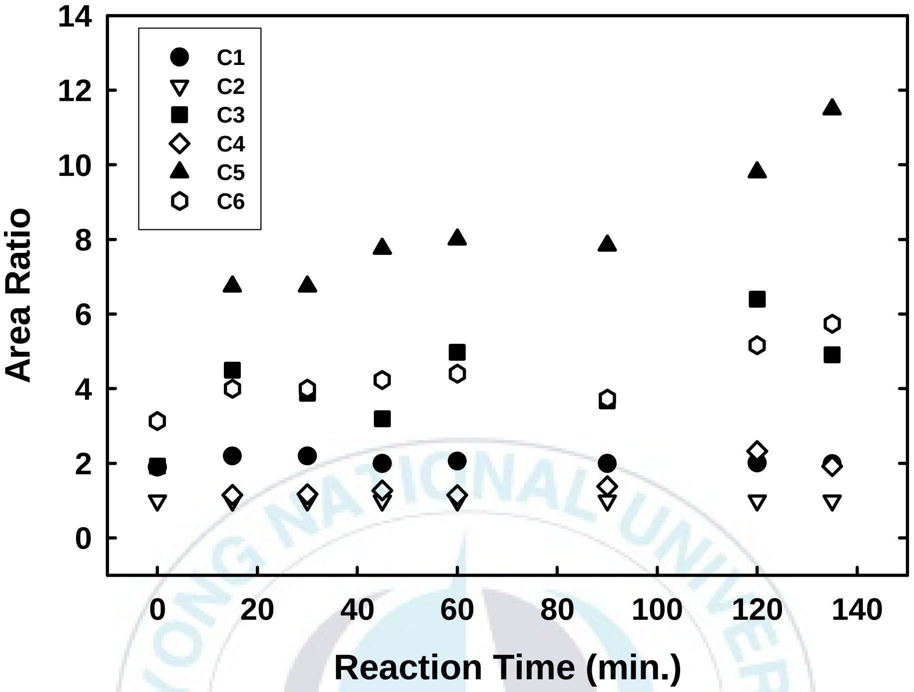

Figure 13. Integrated areas of C1s photoelectron in different chemical environments determined from the spectra such as those in Figure 11 (a) and (b).

2. Pure RTILs study

Figure 14 shows the detailed C1s XP spectra of four pure RTILs, 1-butyl-3-methylimidazolium hexafluorophosphate ([bmim][PF_6]), 1-butyl-3-methylimidazolium tetrafluoroborate ([bmim][BF_4]), 1-butyl-3-methylimidazolium trifluoromethanesulfonate ([bmim][OTf]) and 1-ethyl-3-methylimidazolium tetrafluoroborate ([emim][BF_4]). It was assigned that the binding energies of C1s photoelectron of each deconvoluted peaks based on the chemical environment of the carbons, and labeled the carbons according to the binding energy of C1s photoelectron from high to low.

The ratio from experimental results (1.97:1.00:1.87:3.01) is well matched with the number of carbons in of [bmim][PF_6], 2:1:2:3, within experimental error. The ratios of [bmim][BF_4], [bmim][OTf], [emim][BF_4] are 2.00:1.00:1.99:2.99, 0.78:2.01:1.00:2.04:3.08 and 1.95:1.00:1.97:0.99 respectively. Those experimental results also well matched with the number of carbons (2:1:2:3, 1:2:1:2:3 and 2:1:2:1, respectively) in each RTIL.

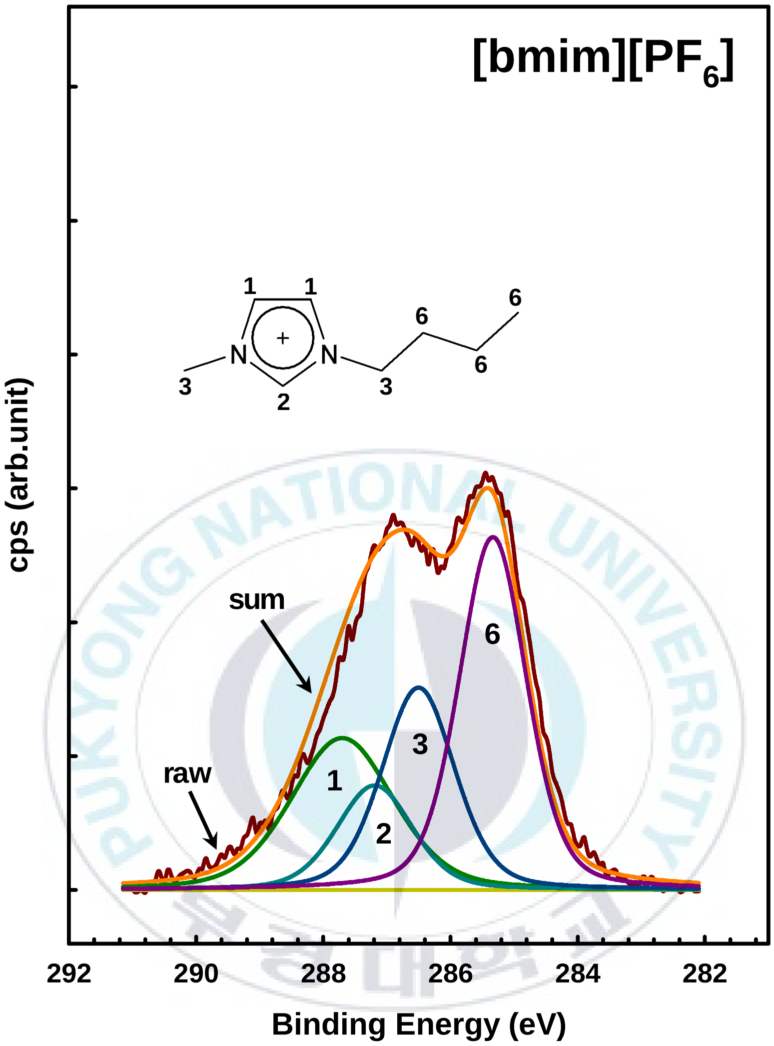

Figure 14. (a) Detailed C1s photoemission of pure [bmim][PF$_6$]. Top two peaks are sum of deconvoluted C1s (smooth line) and raw data (wiggled line). The inset shows the chemical structure of 1-*n*-butyl-3-methylimidazolium cation. (Area ratio 1.97:1.00:1.87:3.01)

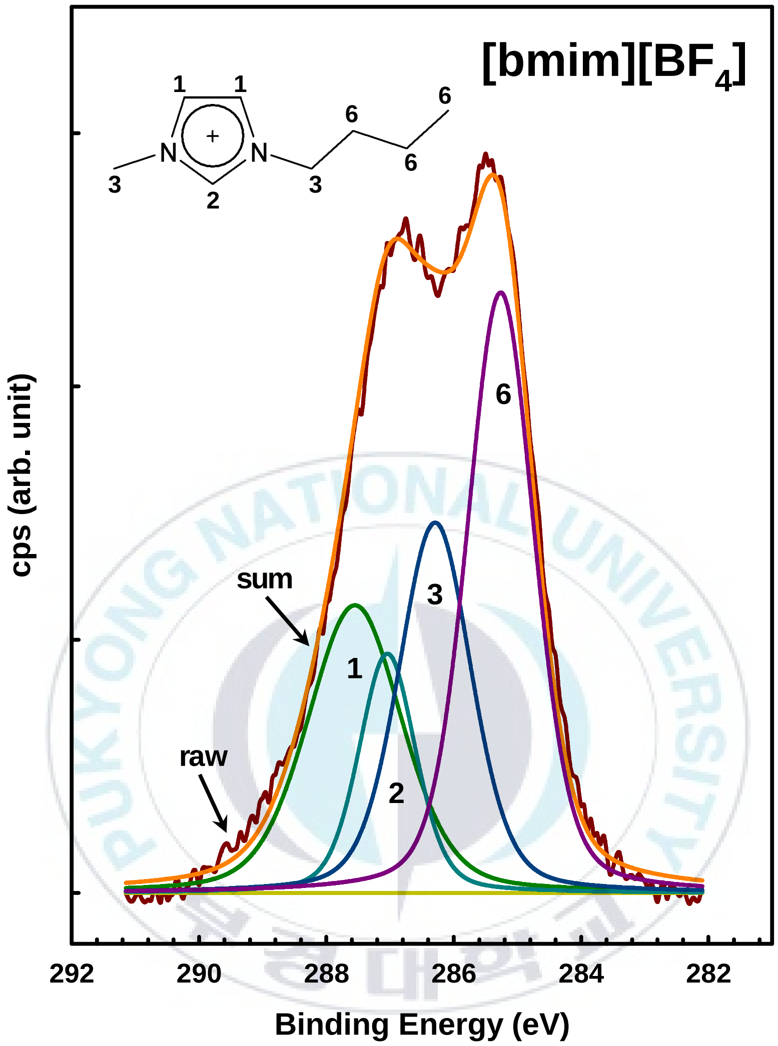

Figure 14. (b) Detailed C1s photoemission of pure [bmim][BF$_4$]. Top two peaks are sum of deconvoluted C1s (smooth line) and raw data (wiggled line). (Area ratio 2.00:1.00:1.99:2.99)

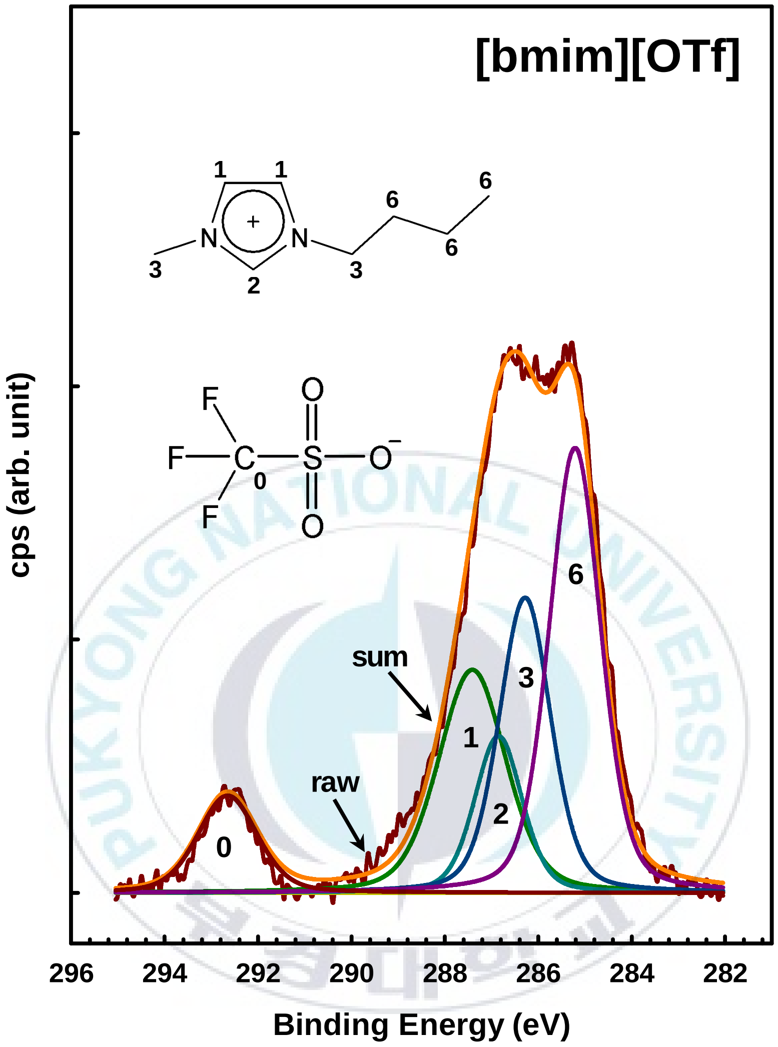

Figure 14. (c) Detailed C1s photoemission of pure [bmim][OTf]. Top two peaks are sum of deconvoluted C1s (smooth line) and raw data (wiggled line). The inset shows the chemical structure of trifluoromethanesulfonate anion. (Area ratio 0.78:2.01:1.00:2.04:3.08)

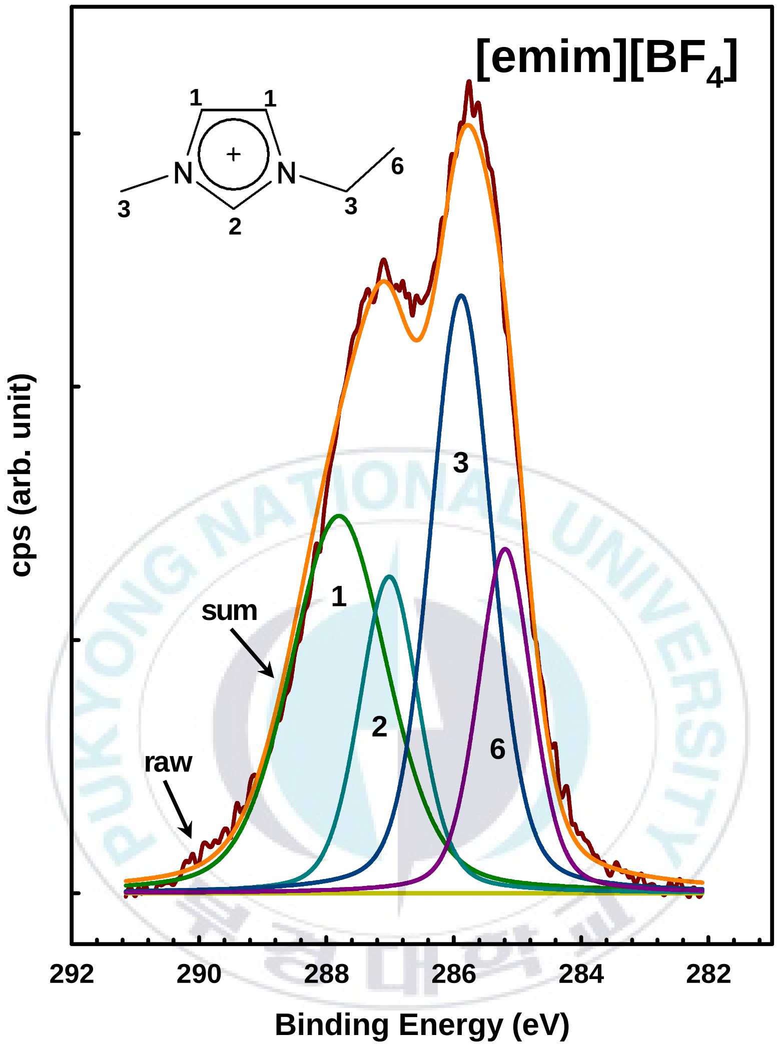

Figure 14. (d) Detailed C1s photoemission of pure [emim][BF_4]. Top two peaks are sum of deconvoluted C1s (smooth line) and raw data (wiggled line). The inset shows the chemical structure of 1-*n*-ethyl-3-methylimidazolium cation. (Area ratio 1.95:1.00:1.97:0.99)

Ⅴ. Conclusion

In this thesis, an organic compound **1**, which was obtained by A^3 coupling using [bmim][PF_6] as a solvent, was characterized in a RTIL solution by XPS analysis without any purification processes. This analytical application is a new field to identify organic compounds with relatively high boiling points in RTILs. The ratio of integrated areas of deconvoluted C1s peaks was well matched to the number of non-equivalent carbons in propargylamine as well as a RTIL within experimental error. Other pure RTILs were also identified using XPS in UHV. These results are expected to provide an important tool and a new strategy for the analysis of organic molecules.

Ⅵ. Reference

[1] J. C. Vickerman (Ed.), Surface Analysis - The Principal Techniques, John Wiley and Sons, Chichester, 1998.

[2] C. Briggs, M.P. Seah (Eds.), Practical Surface Analysis - second edition vol1 : Auger and X-ray photoelectron spectroscopy, John wiley and Sons, Chichester, 1996.

[3] A. Shchukarev, Adv. Colloid Interface Sci. 112 (2006) 149.

[4] M. Faubel, B. Steiner, J. P. Toennies, J. Chem. Phys. 106 (1997) 9013.

[5] B. Winter, R. Weber, P. M. Schmidt, I. V. Hertel, M. Faubel, L. Vrbka, P. Jugwirth, J. Phys. Chem. B 108 (2004) 14558.

[6] D. F. Ogletree, H. Bluhm, G. Lebedev, C. S. Fadley, Z. Hussain, M. Salmeron, Rev. Sci. Instrum. 73 (2002) 3872.

[7] M. A. Henderson, Surf. Sci. Rep 46 (2002) 1.

[8] J. Lukas, R. N. Sodhi, M. V. Seften, J. Colloid Interface Sci. 174 (1995) 421.

[9] A. Gelabert, O. S. Pokrovsky, J. Schott, A. Boudou, A. Feurtet-Mazel, J. Mielczarski, E. Mielczarski, N. Mesmer-Dudons, O. Spalla, Geochim Cosmochim Acta 68 (2004) 4039.

[10] M. Ramstedt, B. M. Andersson, A. Shchukarev, S. Sjöberg, Langmuir 20 (2004) 8224.

[11] A. Shchukarev, S. Sjöberg, Surf. Sci. 584 (2005) 106.

[12] P. Yu, Y. Lin, L. Xiang, L. Su, J. Zhang, L. Mao, Langmuir 21 (2005) 9000.

[13] B. K. Price, J. L. Hudson, J. M. Tour, J. Am. Chem. Soc. 127 (2005) 14867.

[14] E. F. Smith, I. J. V. Garcia, D. Briggs, P. Licence, Chem. Commun. (2005) 5633.

[15] R. Fortunato, C. A. M. Afonso, J. Benavente, E. R. Castellón, J. G. Crespo, J. Membr. Sci. 256 (2005) 216.

[16] S. Caporali, U. Bardi, A. Lavacchi, J. Electron. Spec. Rel. Phen. 151 (2006) 4.

[17] G. S. Fonseca, G. Machado, S. R. Teixeira, G. H. Fecher, J. Morais, M. C. M. Alves, J. Dupont, J. Colloed Interface Sci. 301 (2006) 193.

[18] U. Bardi, S. P. Chenakin, S. Caporali, A. Lavacchi, I. Perissi, A. Tolstogouzov, Surf. Interface Anal. 38 (2006) 1768.

[19] O. Hofft, S Bahr, M. Himmerlich, S. Krischok, J. A. Schaefer, V. Kempter, Langmuir 22 (2006) 7120.

[20] C. W. Scheeren, G. Machado, S. R. Teixeira, J. Morais, J. B. Domingos, J. Dupont, J. Phys. Chem. B 110 (2006) 13011.

[21] E. F. Smith, F. J. M. Rutten, I. J. Villar-Garcia, D. Briggs, P. Licence, Langmuir 22 (2006) 9386.

[22] D. E. Karymann, M. Nouruzian, H. Henze, Synlett (1996) 1091.

[23] A. J. Carmichael, M. J. Earle, J. D. Holbrey, P. B. Mc Lormac, K.R. Seddon, Org. Lett. 1 (1999) 997.

[24] L. Xu, W. Chen, J. Xiao, Organometallics 19 (2000) 1123.

[25] N. Jain, A. Kumar, S. Chauhan, M. S. Chauhan, Tetrahedron 61 (2005) 1015.

[26] D. W. Armstrong, L. K. Zhang, L. He, M. L. Gross, Anal. Chem. 73 (2001) 3679.

[27] M. Mank, B. Stahl, G. Boehm, Anal. Chem. 76 (2004) 2938.

[28] D. Bungert, S. Bastian, D. M. Heckmann-Pohl, F. Giffhorn, E. Hinzle, A. Tholey, Biotechnol. Lett. 26 (2004) 1025.

[29] J. A. Whitehead, G. A. Lawrance, A. McCluskey, Aust. J. Chem. 57 (2004) 151.

[30] K. A. Fletcher, S. Pandey, J. Phys. Chem. B 107 (2003) 13532.

[31] S. Pandey, Anal. Chim. Acta. 556 (2006) 38.

[32] P. Wasserscheid, W. Keim, Angew. Chem. Int. Ed. 39 (2000) 3772.

[33] J. Dupont,R. F. De Souza, P. A. Suarez, Chem. Rev. 102 (2002) 3667.

[34] S. Doherty, P. Goodrich, C. Hardacre, H. K. Luo, D. W. Rooney, K. R. Seddon, P. Styring, Green Chem. 6 (2004) 63.

[35] S. B. Park, H. H. Alper, Chem. Commun. (2005) 1315.

[36] J. F. Watts, J. Wolstenholme (Eds.), An Introduction to SURFACE

ANALYSIS by XPS and AES, John Wiley and Sons, Chichester, 2002.

[37] G. C. Smith (Ed.), Surface Analysis by Electron Spectroscopy - Measurement and Interpretation, Plenum Press, 1994.

[38] Y. W. Chung (Ed.), Practical Guide To SURFACE & SCIENCE SPECTROSCOPY, Academic Press, 1990.

[39] R. Sheldon, Chem. Commun. (2001) 2399.

[40] P. Bonhôte, A. -P. Dias, N. Papageorgiou, K. Kalyanasundaram, M. Grätzel, Inorg. Chem. 35 (1996) 1168.

[41] T. Nishida, Y. Tashiro, M. Yamamoto, J. Fluorine Chem. 120 (2003) 135.

[42] C. P. Fredlake, J. M. Crosthwaite, D. G. Hert, S. N. V. K. Aki, J. F. Brennecke, J. Chem. Eng. Data 49 (2004) 954.

[43] L. P. N. Rebelo, J. N. C. Lopes, J. M. S. S. Esperanç, E. Filipe, J. Phys. Chem. B 109 (2005) 6040.

[44] T. Welton, Chem. Rev. 99 (1999) 2071.

[45] L. Shi, Y. -Q. Tu, M. Wang, F. -M. Zhang, C. -A. Fan, Org. Lett. 6 (2004) 1001.

[46] B. V. Crist (Ed.), Handbook of Monochromatic XPS Spectra: Polymers and Polymers Damaged by X-rays, John Wiley and Sons, Chichester, 2000.

[47] Z. Meng, A. Dölle, W. R. Carper, J. Mol. Struct. (Theochem) 585 (2002) 119.

Ⅶ. Appendix

Procedure of XPS (VG ESCALAB 2000)

1. Sample installing

(1) Push the **'PUMP Fast Entry Air Loadlock (FEAL)'** button "off".

(In order to vent the preparation chamber, wait 2~3 minutes)

(2) Open the N_2 gas cylinder.

(In order to minimize the contamination of UHV chamber from other gases)

(3) When the door of FEAL chamber opens, put the sample into the sample stub holder, and then close the door.

(4) Close the N_2 gas cylinder.

(5) Push the **'PUMP FEAL'** button "on".

(6) Wait for decreasing the pressure in preparation chamber (1~2 hours).

(7) Open Main Gate Valve (MGV) slowly. Checking the pressure inside of the XPS chamber.

(8) Push the sample into the main chamber by using magnetic transfer rod.

(9) **!!!Careful!!!** Mount the sample on the manipulator by using a wobble stick which is installed in the analysis chamber.

(10) Pull the magnetic transfer rod out, and then close the MGV.

(11) Set the sample in position by using the manipulator (x, y, z, Θ) watching CCD camera monitor.

(12) Down the X-ray source checking distance from the sample with care.

(13) Turn on the chiller (to cool down X-ray source).

2. Analyser Setting (User Setup Page)

(1) **'User Setup Pages'** (icon) click

(2) Lens mode change (SAXPS or LAXPS), knob of XPS chamber check (SAXPS : 8.5 or LAXPS : 0), and then **'Apply'** click

3. Avantage operating

(1) **'Avantage'** (icon) click

(2) File - Open Experiment : sequence change

< **Survey scan** >
Energy scale : Binding
Pass mode : CAE
Energy ranges : AES/XPS
Start Energy : 0 eV
End Energy : 1100 eV
Pass Energy : 50 eV
Number of Scans : 1
Dwell Time : 50 ms
Energy Step Size : 1 eV
Lens Mode : Large Area

< **Narrow scan** >

< **C1s** >

Start Energy : 272 eV
End Energy : 300 eV
Pass Energy : 20 eV
Number of Scans : 3
Dwell Time : 50 ms
Energy Step Size : 0.05 eV

* **Start and End Energy** of each atom refer to the **Data Book.**
In this experiment, energy ranges used are N1s (390~415 eV), F1s (675~695 eV), P2p (125~145 eV), O1s (520~545 eV), Cu2p(925~965 eV).

4. X-ray sources controlling

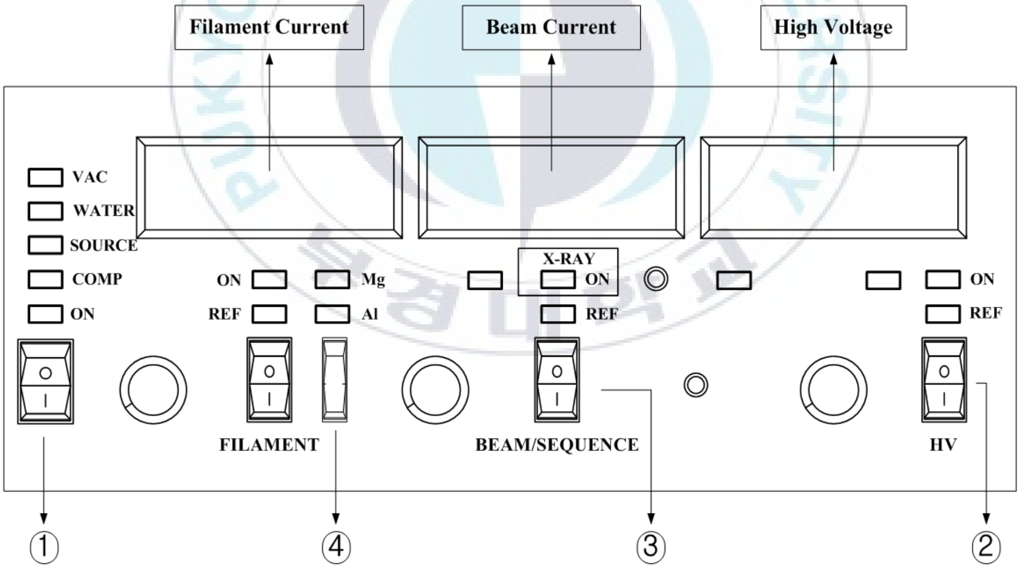

(1) Turn on amin power by pushing the ① button and checking all LED lights on above the ① button (green is normal).

(2) Turn on the High Voltage (HV) by pushing ② button.

(3) When the HV is approximately 15 kV, turn on beam energy by

pushing the ③ button.

(4) Check the Filament Current and the Beam Current.
(approximately 4.4 A and 15 mA)

(5) If you want to change the X-ray source, push the ④ button.

5. Scan Starting (in Avantage)

(1) Click Experiment run (▶ : green color) icon.

(2) Click New processing view ▦ icon.

(3) Drag survey and narrow scan windows on the new processing view window.

(4) Save data and convert the Avantage data into EXCEL data.
(by copy active cell - by clicking the right mouse button on the active window)

6. Turn off process

(1) Turn off X-ray source by pushing ③ button.

(2) Turn off HV by pushing ② button and ① button.

(3) Lift up the X-ray source with care.

7. The Sample take out

(1) Open the MGV and carefully move the magnetic transfer rod in.

(2) Mount the sample on the magnetic transfer rod by using wobble stick.

(3) Pull the magnetic transfer rod out and close the MGV.

(4) Turn off the chiller.

(5) Vent the preparation chamber for taking out the sample.

Korean Abstract

초고진공 (UHV) 에서의 상온 이온성 액체의 X-선 광전자 분광학(XPS) 연구

권지혜

부경대학교교육대학원 화학교육전공

요 약

상온 이온성 액체 내에서의 유기분자들의 확인을 위해 새로운 분석 기술인 XPS의 이용을 보고한다. 상온 이온성 액체 (RTILs)의 하나인 1-butyl-3-methylimidazolium hexafluorophosphate ([bmim][PF_6]) 용매 내에서 A^3 결합 반응을 통해 합성된 유기화합물인 propargylamine (1)을 NMR과 같은 전통적인 유기화합물 분석 기술을 사용하기보다 X-선 광전자 분광법 (XPS)을 이용해 분석하였다. RTIL와 1 각각에는 네가지 동등하지 않은 탄소들이 존재한다. 탄소 (C1s) peak들의 핵심부 전자들의 결합에너지를 화학적 환경에 의해 분리한 peak의 영역들의 비는 이 화합물들에 존재하는 탄소들의 수와 잘 일치된다. (1)의 분리된 탄소 peak들 중 C4 (아세틸렌 그룹의 sp탄소)와 C5 (벤젠 링의 sp^2탄소)의 결합에너지는 각각 286.2와 285.4 eV로 부여 하였다. 우리는 또한 몇 가지 순수한 상온 이온성 액체를 UHV에서 XPS를 사용하여 분석하였다. 이러한 결과들은 유기화합물의 분석을 위한 중요한 도구와 새로운 방법을 제공할 수 있을 것이다.

Acknowledgment

I would like to express my gratitude and indebtedness to the many special people who in one way or another contributed to the success of this thesis.

First of all, I would like to thank my advisor, Prof. Yong-Cheol Kang, for his trustful guidance, expert advice and encouragement. I would also like to extend my gratitude to all my thesis committee members, Prof. Ju Chang Kim and Prof. So Won Youn, for their valuable time and helpful comments.

I also thank to all graduate students, Young Hwa Kim, Im Sung Shin, Hye Yoon Jung, Han Young Park, Eun Ju Cho, Hyoun Jung Seok and Gyung Seon Oh, for sharing delight and trouble with me for two and a half years. I would deeply appreciate to friends all my life: Kwang Ho Lee, Yong In Kim, Hwi Young Ko, Young Ju Kang, Sung Su Kim, Eun Ju Kim, Hee Won Kim and Chae Duk Jung. And I would like to express thanks to junior members of Surface Analysis Laboratory: Ju Yun Park, Se Won Jung and Mi Sun Chun.

I would like to thank my friends for their friendship, and others who I have unintentionally forgot to mention for the times we shared.

Lastly, I owe special thanks to my parents, younger sister and brother for their continuous care, inspiration and support.

August 2007

Ji Hye Kwon